polysaccharides

MDPI

Article

Optimization of the Mechanical Isolation Process of Mucilage from Chia Seeds (*Salvia hispanica* L.): Physicochemical, Morphological, and Rheological Characterization

Frida R. Cornejo-García [1,2], Ricardo M. González-Reza [1], Isela Rojas-Molina [3], Adriana Rojas-Molina [4], José L. Sánchez-Millán [1], Carlos T. Quirino-Barreda [2] and Elsa Gutiérrez-Cortez [1,*]

[1] Laboratorio de Procesos en Ingeniería Agroalimentaria, Facultad de Estudios Superiores Cuautitlán, Universidad Nacional Autónoma de México, Cuautitlán Izcalli 54714, Estado de México, Mexico; frida.cornejo.g@comunidad.unam.mx (F.R.C.-G.); gonzalez.reza@comunidad.unam.mx (R.M.G.-R.); jlsan@unam.mx (J.L.S.-M.)

[2] División de Ciencias Biológicas y de La Salud, Departamento de Sistemas Biológicos, Universidad Autónoma Metropolitana, Coyoacán 04960, Ciudad de México, Mexico; cquirino@correo.xoc.uam.mx

[3] Laboratorio de Química Medicinal, Facultad de Química, Universidad Autónoma de Querétaro, Cerro de las Campanas S/N, Santiago de Querétaro 76017, Querétaro, Mexico; isela.rojas@uaq.mx

[4] Laboratorio de Visualización de Datos DATALAB, Facultad de Ingeniería, Universidad Autónoma de Querétaro, Santiago de Querétaro 76010, Querétaro, Mexico; adriana.rojas@uaq.edu.mx

* Correspondence: elsane@comunidad.unam.mx; +52-55-5623-1999 (ext. 39404)

Abstract

This study aimed to evaluate how hydration temperature, rotational speed, and screw restriction influence the extraction efficiency, physicochemical characteristics, and monosaccharide composition of chia seed mucilage (CSM). Optimal extraction conditions (43.7 Hz, 100% screw restriction and 50 °C) yielded an extraction efficiency of 65.69% and a mucilage yield of 7.66%, producing a material with an average particle size of 15.28 µm, a ζ-potential of 9.7 mV, and weak-gel rheological behavior. Structural analyses confirmed the absence of insoluble fiber and revealed crystalline phases including MgO, Ca_5P_8, K_2S, K_4P_6, and $CaCO_3$, along with typical polysaccharide functional groups (–OH, –CH, C=O, COO^-, C–O). Moderate hydration temperature combined with controlled mechanical conditions favored the release of mucilage enriched in xylose, glucose, and arabinose, which are characteristic of seed coat polysaccharides. In contrast, minimal mechanical action or excessive seed disruption shifted the monosaccharide profile toward cell wall structural carbohydrates, indicating reduced mucilage purity. Elevated hydration temperature (75 °C) enhanced the solubilization of uronic acids and arabinose, suggesting increased extraction of acidic polysaccharide fractions associated with the seed coat matrix. These findings demonstrate that extraction parameters strongly determine CSM composition, structural integrity, and functional attributes. The results provide a basis for tailoring chia-derived polysaccharides for applications in hydrocolloid systems, bio-based materials, and functional polymer formulations.

Keywords: Box–Behnken design; centrifugation conditions; food hydrocolloid; separation efficiency; yield

Check for updates

Academic Editors: Elisabete Coelho and Janusz Kapusniak

Received: 5 November 2025
Revised: 9 March 2026
Accepted: 8 April 2026
Published: 11 April 2026

Copyright: © 2026 by the authors. Licensee MDPI, Basel, Switzerland. This article is an open access article distributed under the terms and conditions of the Creative Commons Attribution (CC BY) license.

1. Introduction

The *Salvia hispanica* L. (chia) seed is composed of pericarp or hull, testa, endosperm, and an embryo with two cotyledons. The outer layer of the testa is composed of thin-walled polygonal cells that contain mucilage. When chia seeds come into contact with

water, the exocarp swells, and its elasticity is lost when the cuticle ruptures. The epicarp cells, primarily made of mucilage, are released into the surrounding medium; this is known as chia seed mucilage (CSM) [1]. In chia seeds, mucilage appears as a thick, gelatinous substance that surrounds the seeds after hydration and is very rich in carbohydrates. These polysaccharides, which make up the mucilaginous network, are found in the three outer layers of the seed coat, forming the testa [2,3]. CSM has a molecular weight between 800 and 2000 kDa. It consists of heteropolysaccharides composed of monosaccharides such as D-xylose, D-mannose, L-arabinose, D-glucose, galacturonic acid, and glucuronic acid [4,5].

CSM exhibits excellent properties as an emulsifier, stabilizer, and water retention agent due to the viscosity it develops in aqueous media [6,7]. Therefore, it has been successfully incorporated into baked goods, dairy products, and meat products. It also improves the textural properties of products where it is used as a substitute for egg, gluten, and other ingredients [8]. Given its significant impact on the incorporation of various products, its extraction and purification are of utmost importance in the food industry. CSM extraction involves three stages: hydration, separation, and recovery [8]. There are different ways to obtain CSM regardless of the separation method used, including emerging technologies [6,9] such as microwave-assisted extraction, ultrasound-assisted extraction, pulsed electric field extraction, and so on [10–14]. All these methods evaluate process characteristics such as the yield obtained from the applied separation, as well as the purity of the polysaccharide obtained, which can significantly impact its rheological, functional, thermal, physicochemical, and pasting properties [15]. However, these processes can be costly, so implementing methods that achieve high purity and separation efficiency is crucial at the industrial level [14]. Research into optimizing CSM separation conditions is key to adequately describing the process and enabling its industrial application [16,17].

While there are extensive studies on the optimization of CSM extraction conditions, it is important to note that this research reports for the first time the optimal extraction conditions for CSM using a disk centrifuge. This process was chosen because it separates the components quickly and easily and allows for greater separation efficiency, thus obtaining mucilages with fewer impurities than other components of the seed. Therefore, the objective of this experimental work was to optimize process conditions for ultrahigh centrifugation extraction, evaluating the limits of process variables such as hydration temperature, rotation speed, and screw position for the extraction of mucilage from *S. hispanica* L. seeds. Response variables such as yield and extraction efficiency were also evaluated using a Box–Behnken design. Furthermore, the influence of these variables on the chemical, physical, physicochemical, and rheological properties of the mucilage obtained from *S hispanica* L. seeds was established.

2. Materials and Methods

2.1. Optimization of the Mucilage Extraction Process

The seeds of *S. hispanica* L. were obtained from experimental fields of the University of Chapingo, Mexico. The coordinates of the crop area were Lat N 19°29′, Longitude 98°53′, Altitude 2250 m. A Box–Behnken design was used to evaluate the effect of the factors CSM extraction process [turning speed (X_1), restriction of screw (X_2) and hydration temperature (X_3)] on the yield (Y_1) and efficiency of separation (Y_2). Table 1 shows the factors and their levels that were established based on preliminary activities.

All experiments were carried out considering three replications and in random order. The coefficients of the response surface equation were determined, an analysis of variance (ANOVA) was performed to evaluate any significant differences between the independent variables ($\alpha = 0.05$), and the optimum conditions for the mechanical isolation process of mucilage from chia seeds were determined by applying a desirability function (D) [18]

All statistical analyses were performed using the Minitab statistical program (Minitab® Statistical Software 19 Inc., Centre, PA, USA).

Table 1. Uncoded and coded independent variables used in Box–Behnken design.

Coded Variables	Uncoded Variables	Coded Levels		
		−1	0	1
X_1	Turning speed (Hz)	31.25	37.5	43.75
X_2	Restriction of screw (%)	0	50	100
X_3	Hydration temperature (°C)	25	50	75

Following previous reports related to CSM extraction at different processing conditions, the extraction yield and efficiency were optimized with a response surface analysis to maximize the response according to the model. To assess the model reliability, four additional tests were performed around the optimal operating conditions, agreeing with selecting an optimal design according to the results obtained [19]. Figure 1 shows the process diagram with operating conditions for the mucilage extraction process.

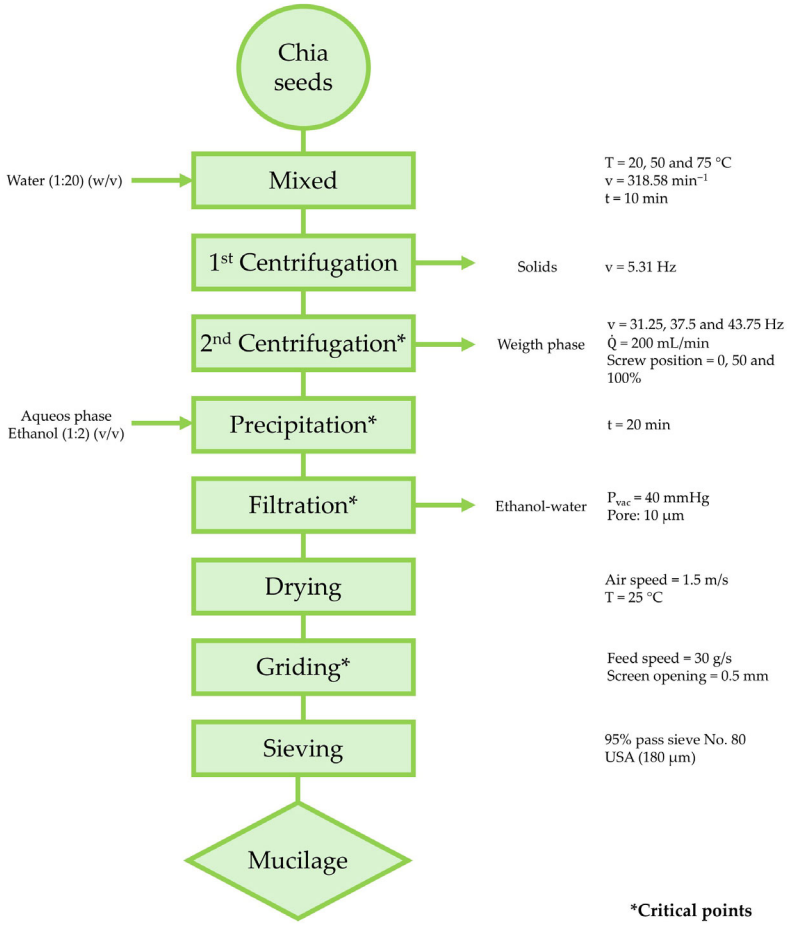


Figure 1. Diagram of the process of extracting *S. hispanica* L. mucilage.

Figure 1 shows the process diagram for the mechanical isolation process of mucilage from *Salvia hispanica* L. seeds. In a mixer tank equipped with a marine propeller (IKA-WERKE, Mod. Eurostar BSC.S1, Wilmington, NC, USA), 20 L of distilled water were added and heated at three temperatures according to experimental design. Later, 1 kg of *S. hispanica* L. (chia) seeds were added in a seed–water ratio of 1:20 (*w*/*v*) in each case. The mixture was homogenized at 318.58 min^{-1} for 5 min. The mix was cooled for 5 h until reaching 25 °C. Subsequently, the viscous fluid was partially separated from the seeds into a basket

centrifuge (TURMIX Mod. M-02, Ocoyoacac, Edo. de México, México) at 2.18 Hz. The fluid that flowed out of the basket centrifuge was transferred to a disk centrifuge (Didacta Italia, Mod.TAG1/d, Torino, TO, Italy) at a constant feed speed of 200 mL/min and centrifuged. The turbidity was analyzed with a turbidimeter (Hanna LP 2000, Nusfalau, Romania) by the method 1889-88a ASTM (2012) [20]. In addition, extraction efficiency was evaluated by using the turbidity according to the following Equation (1):

$$\text{Extraction efficiency } (\%) = [(t_s - t_{fl})/t_s] \times 100 \quad (1)$$

where t_s = turbidity of the suspension placed in the centrifuge (NTU) and t_{fl} = turbidity of the aqueous phase (NTU).

The aqueous phase was added with ethanol 96 °GL: ethanol 1:2 (*v*/*v*) ratio to induce mucilage precipitation; this was a critical step in the extraction process. The mucilage was separated by using a vacuum filtration system at 5.33 kPa with a filtering medium (70–30% polyester–cotton) with a pore size of 10 µm. The mucilage was dehydrated until it reached a moisture of 4% with forced air at room temperature. Then, this material was ground in a blade mill (Thomas-Wiley Laboratory Mill, Model 4, Thomas Scientific, Swedesboro, NJ, USA) with a 0.5 mm mesh at the output restriction.

This was a critical point too, because the particle size of the granular solid of the mucilage is important for future applications. Also, these measurements were carried out in the aqueous phase and the mucilage powders in aqueous dispersion at concentrations of 0.125, 0.25, and 0.5% (*w*/*w*). The mucilage yield was determined with the following Equation (2):

$$\text{Mucilage yield } (\%) = (W_{CSM}/W_{CS}) \times 100 \quad (2)$$

where W_{CSM} = mucilage weight (g) and W_{CS} = *S. hispanica* L. seeds weight (g).

2.2. Chemical Proximate Analysis of CSM

Proximal analysis of powder mucilage was determined according to the Official Methods of Analysis of AOAC International (2012) [21]. Moisture (Method 934.01); ash (Method 923.03); protein (Method 984.13) by 6.25 as a factor to quantify N total; lipids (Method 920.39), and fiber (Method 925.09). The carbohydrate content was obtained by the difference in the other components.

2.3. Assessment of Monosaccharide Profile of Chia Seed Mucilage by High-Performance Liquid Chromatography (HPLC)

The monosaccharide content (glucose, galactose, mannose, and xylose) of the samples was determined according to the procedure described by Timilsena et al. [22], with minor modifications. Briefly, 100 mg of each sample were hydrolyzed with 10 mL of 1 mol H_2SO_4 at 95 °C for 24 h in sealed tubes. Following hydrolysis, the samples were centrifuged at 10,000× *g* for 15 min, and the resulting supernatant was neutralized to pH 7 using 1 mol NaOH. The suspension volume was then adjusted to 50 mL with Milli-Q water (Millipore Corporation, Billerica, MA, USA). The solutions were filtered through membrane filters prior to chromatographic analysis. Monosaccharide profiling (xylose, glucose, glucuronic acid, arabinose, mannose, and galactose) was performed using a high-performance liquid chromatography (HPLC) system (Waters Co., Milford, CT, USA; Model e2695) equipped with a refractive index detector (Waters Co., Milford, CT, USA; Model 2414). Separation was carried out on a Waters NH_2 analytical column (4.6 mm × 250 mm, 5 µm) maintained at 80 °C. An isocratic elution system composed of acetonitrile and water (75:25 *v*/*v*) was employed, with a total run time of 23 min. The injection volume was 20 µL, and the mobile phase flow rate was set at 1.5 mL/min. Monosaccharides were identified by comparing

retention times with authentic standards (Sigma Chemical Co., St. Louis, MO, USA), and quantification was accomplished using external calibration curves. All measurements were performed in triplicate.

2.4. Molecular Weight (MW) Estimation

The molecular weight (MW) of the CSM was estimated by capillary viscometry following the methodology reported by Timilsena et al. [23]. Briefly, 0.25 g of dry chia mucilage was dissolved in 250 mL of a buffer solution, the solution was filtered. Subsequently, chia mucilage dilutions were prepared using deionized water (0.01, 0.02, 0.03, 0.04, 0.05 gdL^{-1}) for the samples (1 to 5). The viscosity of each dilution was measured using an Ostwald-type capillary viscometer (Oswald-type viscosimeter, Schott, Mainz, Germany) immersed in a water bath at 25 °C. The fall times of the buffer solution (t_0) and the biopolymeric solutions (t) were measured, and three measurements were performed for each sample. The relative, specific, and reduced viscosities were calculated to obtain the intrinsic viscosity. The average MW was estimated according to the Mark–Houwink Sakurada (MHS) equation, which relates the inherent viscosity of a polymer solution with the molecular weight of the polymer, using a value of a = 0.8 by Timilsena et al. [23] and Masuelli [24].

2.5. X-Ray Fluorescence Spectrometry (FRX)

The first method used to determine the inorganic components in the mucilage was determined by X-ray fluorescence spectrometry, in the incinerated samples, according to ASTM (2012). The ash samples were placed in a Bruker spectrometer S2 PUMA (Billerica, MA, USA) to be evaluated.

2.6. Identification of Crystalline Structures in CSM by X-Ray Diffraction (XRD)

The samples of CSM were analyzed by an XRD diffractometer (Rigaku Ultima IV, Tokyo, Japan) with operating conditions of 40 kV and 30 mA, with a CuKα radiation wavelength of 1.5406 Å. The powder (ashes) from the incinerated samples were densely packed in an aluminum sample holder. The measurements were performed from 5 to 80° on a 2θ scale with a step of 0.02 following the methodology proposed by [25].

2.7. Flow Properties of CSM

The density of the CSM granular solids of the selected samples was determined. The compressibility of mucilage powder was determined by the Carr index (CI). The flowability capacity of granular material was established through the Hausner index (FH).

2.8. Morphological Characterization of S. hispanica L. Seeds and CSM by Scanning Electron Microscopy

The morphology of the hydrated *S. hispanica* L. seeds and CSM was studied in a Low Vacuum Scanning Electron Microscope (SEM-LV) (Jeol JSM 6060LV, Tokyo, Japan). The CSM in a piece was placed on an aluminum surface with carbon, and it was fixed to the sample holder and covered with a gold bath for its observation. The analysis was developed at an acceleration of electrons of 20 kV and a pressure of 10–20 Pa in each chamber. The micrographs were obtained on the sample surface.

2.9. Fourier Transform Infrared Spectroscopy (FTIR) Analysis of CSM

The CMS samples were analyzed by using an FTIR Spectrum Two Instrument (Perkin Elmer, Überlingen, Germany) with ATR (Attenuated Total Reflectance). The transmittance values were recorded at different wavelengths from 600 to 4000 cm^{-1} to acquire the chemical spectra and detect modifications in mucilage constituents due to the extraction process conditions.

2.10. Refraction Index, pH, and Particle Size Distribution in Mucilage Dispersions

Mucilage dispersions were prepared at concentrations of 0.25, 0.5, and 1% (*w*/*v*) in deionized water. At a temperature of 25 °C and 170 rpm of stirring for 30 min. The pH was measured in a potentiometer (Model HI9811-5, Hanna Instruments, Limena, Italy), refraction index (RI) was determined in a refractometer (Abbemat MW, Anton Paar GmbH, Graz, Austria). The particle size distribution (PSD) was measured by a laser scattering PSD analyzer (LA-960, Horiba, Kyoto, Japan) using 1.60 as a relative refractive index.

2.11. Zeta Potential (ζ)

The zeta potential of CSM dispersions reflects particle charge and may be influenced by other particles and the composition of the medium. The CSM sample was dispersed in water at concentrations of 0.25%, 0.5%, and 1% (*w*/*w*). These solutions were steeped for 24 h to evaluate the stability of mucilage aggregation by measuring zeta potential using a zetasizer 3000 (Malvern Instrument Inc., London, UK). The mucilage dispersion at a temperature of 25 °C was introduced into the cell equipment. The equipment containing two electrodes, and an electric field was applied to the electrodes to determine the zeta potential (ζ in mV).

2.12. Rheological Analysis of Mucilage Dispersions

The CSM samples were dispersed in deionized water at concentrations of 0.25, 0.5, and 1% (*w*/*w*) at 25 °C and 170 rpm of stirring for 120 min. The rheological measure of the mucilage was conducted in a rheometer (MCR 102; Anton Paar, Graz, Austria), with a concentric cylinder probe (CC27 SN29767) in the oscillatory mode. The linear viscoelastic region was determined by strain sweep by using a constant frequency of 10 rad/s and deformation from 0.1 to 10%. To evaluate the rheological properties, the storage modulus (G′) and loss modulus (G″) were determined in Pa, were determined with an amplitude sweep in a range from 0.001 to 5 Hz and 2% of strain [26].

3. Results and Discussion

3.1. Data Statistical Processing in the Optimization

Table 2 shows representative experimental lots of heat treatment in the mechanical isolation process of mucilage from chia seeds. These results reveal that experiments 2, 4, 8 and 13 were those with the highest yield of mucilage and extraction efficiency. Initially, in the first separation of the mucilage from the seed, through a basket centrifuge, a yield of 16.23 ± 0.52% was obtained.

Table 2. Batch mean analysis in the optimization of the mucilage extraction process.

Batch No.	Turning Speed (Hz)	Restriction of Screw (%)	Hydration Temperature (°C)	Mucilage Yield (%)	Extraction Efficiency (%)
1	31.25	0	50	3.83 ± 0.03	18.24 ± 1.16
8	43.75	50	75	7.31 ± 0.01	62.18 ± 0.21
4	43.75	100	50	7.89 ± 0.01	63.01 ± 0.03
12	31.25	100	75	6.82 ± 0.09	35.46 ± 0.07
7	31.25	50	75	6.24 ± 0.02	29.57 ± 0.8
2	43.75	0	50	7.19 ± 0.02	61.92 ± 0.11
10	31.25	100	25	5.41 ± 0.15	37.61 ± 0.25
5	31.25	50	25	4.23 ± 0.09	20.67 ± 0.21
13	31.25	50	50	7.14 ± 0.40	37.01 ± 1.76
9	31.25	0	25	5.88 ± 0.06	26.19 ± 0.42

Muñoz et al. [1] reported a yield of 6.9 g/100 g seeds, but the used temperatures were very high; in the present work, temperatures higher than 75 °C were discarded. Capitani et al. [2] reported in the extraction of mucilage, a yield of 3.8 g mucilage /100 g seeds (dry basis). Orifici et al. [19] optimized the extraction process of chia mucilage, and they

analyzed the effect of mechanical agitation time during mucilage extraction to determine the optimal operating combination of temperature and seed: water ratio in the extraction process; these authors reported an extraction yield of 11.6 g/100 g (dry).

The results obtained with ultracentrifugation are significantly higher than those previously reported, highlighting that the conditions reported by other authors are more drastic and that they also do not report separation efficiency, which is a crucial parameter for semi-industrial and industrial scaling. Additionally, García-Salcedo et al. [15] presented images of defatted seeds with spherical bodies corresponding to proteins without the fat cover and surrounded by insoluble fiber. Therefore, the pressed seed and defatted easily expose the fiber and proteins.

Table 3 shows the analysis of variance (ANOVA) for the coefficients of the polynomial regression model obtained in the Box–Behnken design. The result reflects the influence of the factors studied on the function of the experimental data. According to the lack-of-fit test, which represents the behavior of the experimental data at the limits of the experimental design, it adequately described the influence of the factors analyzed on the independent variables.

Table 3. ANOVA and regression coefficients on response variables in the function factors studied.

Term	Mucilage Yield (%)		Extraction Efficiency (%)	
	Coefficient	***p*-Value**	**Coefficient**	***p*-Value**
β_0	7.141 [a]	0.000	37.008 [a]	0.000
β_1	0.9221 [a]	0.000	18.843 [a]	0.000
β_2	0.4908 [a]	0.000	4.643 [a]	0.000
β_3	0.6074 [a]	0.000	0.402 [ns]	0.440
β_{11}	−0.397 [a]	0.005	9.742 [a]	0.000
β_{22}	−0.311 [a]	0.023	−3.426 [a]	0.000
β_{33}	−0.769 [a]	0.000	−3.084 [a]	0.000
β_{12}	−0.576 [a]	0.000	−2.699 [a]	0.001
β_{13}	−0.206 [ns]	0.111	−2.241 [a]	0.004
β_{23}	0.289 [a]	0.028	0.33 [ns]	0.654
R^2	88.08		97.93	
R^2-adj	84.95		97.40	

β_0 = regression coefficient; β_i = lineal coefficient; β_{ii} = quadratics coefficients; β_{ij} = interaction coefficients. [a] significant ($p \leq 0.05$). [ns] not significant ($p > 0.05$).

For mucilage yield, all terms were significant ($p \leq 0.05$), except for the turning speed and hydration temperature interaction term ($p > 0.05$). For extraction efficiency, all terms were significant ($p \leq 0.05$), except for the linear hydration temperature term and the restriction of the screw and hydration temperature interaction term ($p > 0.05$). Consequently, yield varies according to the unit operations used in the extraction process. In the present study, a response surface methodology (RSM) was used for the optimization of the extraction process. It was based on factorial designs that allowed evaluating the effect of the variables: the turning speed (speed) in Hz, hydration temperature (temperature) in °C, and the position of restriction screws in percentage, on the yield and efficiency of mucilage extraction (Figure 2).

Figure 2a,c shows the extraction efficiency of CMS as a function of the variables analyzed. An inflection is observed at the central points of the model, with a maximum at the central levels of hydration temperature and at the axial levels of screw restriction, presenting values above 38% up to an average maximum of 60%. The least squares equation for the second order for mucilage yield (%) (Y_1) of significant terms is as follows:

$$(Y_1) = -23.13 + 1.068\,X_1 + 0.08\,X_2 + 0.185\,X_3 - 1.02 \times 10^{-2} X_{11} - 1.25 \times 10^{-4}\,X_{22} - 1.23 \times 10^{-4}\,X_{33} - 1.843 \times 10^{-3}\,X_{12} + 2.31 \times 10^{-4}\,X_{23} \quad (3)$$

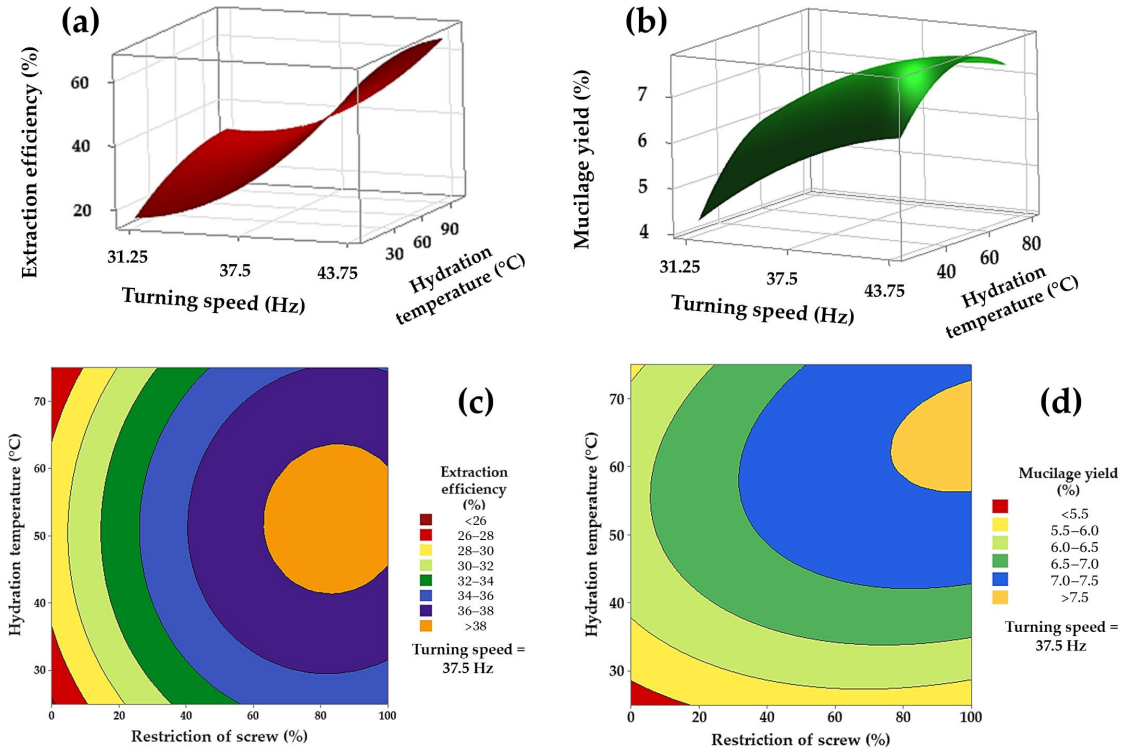


Figure 2. Effect of dispersion–hydration temperature, turning speed, and screw opening of the mucilage extraction process on: (**a**,**c**) extraction efficiency; (**b**,**d**) mucilage yield.

Figure 2b,d shows the CSM yield as a function of the variables analyzed. Maximum yield is observed at the axial points of the model at 60 °C hydration temperature and 100% screw restriction, with average yield values of 7%. The least squares equation for the second order for extraction efficiency (%) (Y_2) of significant terms is as follows:

$$(Y_2) = 211 - 14.54X_1 + 0.541X_2 + 0.249X_{11} - 1.37 \times 10^{-3}X_{22} - 4.93 \times 10^{-3}X_{33} - 8.64 \times 10^{-3}X_{12} - 1.434 \times 10^{-2}X_{13} \quad (4)$$

Optimization for the mechanical isolation process of mucilage from chia seeds was carried out by first superimposing contour plots for extraction efficiency and mucilage yield as a function of turning speed and restriction of the screw at a constant hydration temperature of 50 °C (Figure 3).

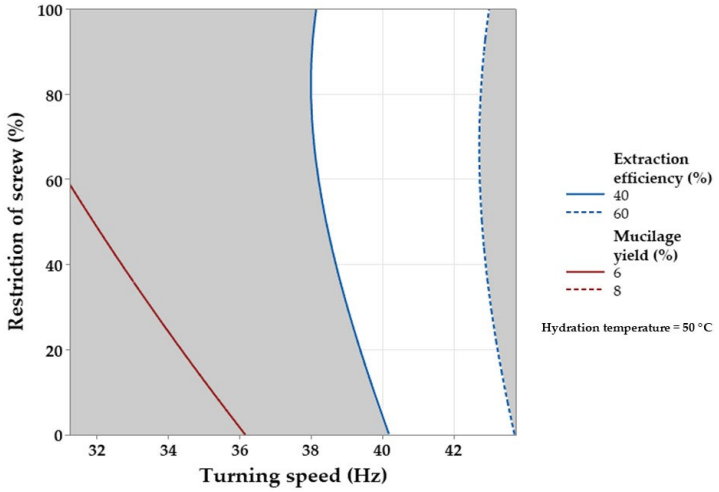


Figure 3. Superimposed contour plot of turning speed and restriction of screw at constant hydration temperature of 50 °C.

A numerical procedure was applied to predict the exact optimal level of the independent variables leading to the desirable function (D) response objectives [18]. The optimal process conditions obtained for the mechanical isolation process of CSM were a turning speed of 43.75 Hz, restriction of the screw of 100%, and hydration temperature of 50 °C, obtaining optimal values of 65.69% for extraction efficiency and yield mucilage of 7.66% (D = 0.9629). To validate the generated quadratic regression model, four additional extraction tests were performed on those obtained in the optimization, this to give robustness to the model, which are shown in Table 4.

Table 4. Batch mean analysis of mucilage yield and extraction efficiency in the optimal design.

Sample	Turning Speed (Hz)	Restriction of Screw (%)	Hydration Temperature (°C)	Mucilage Yield (%)	Extraction Efficiency (%)
1	5.3	0	50	1.2 ± 0.5	4.65 ± 0.9
2	31.25	0	75	3.6 ± 0.1	14.4 ± 0.3
3	43.75	50	75	6.2 ± 0.2	61.3 ± 1.8
4	43.75	100	50	7.7 ± 0.1	67.8 ± 2.1
5	50.2	100	25	8.1 ± 0.3	61.9 ± 1.2

3.2. Proximal Chemical Composition

The proximal chemical composition of the five CSM samples shown in Table 5. The lowest protein content was observed in samples 3 and 4 (2.65 ± 0.05 g/100 g of CSM), while sample 2 had the lowest lipid content. Notably, samples 3 and 4 had low protein content, with 2.65 ± 0.05 g/100 g of CSM, and sample 4 had a lipid content of 0.56 ± 0.03 (g/100 g de CSM). For carbohydrates, sample 3 contained 78.12 ± 0.03 (g/100 g of CSM). The proximal chemical composition of the *S. hispanica* L. mucilage reported by [1] showed a low total carbohydrate content of 48 ± 0.55 g /100 g of CSM and did not report any type of fiber. In the study by [19], 56.33 ± 1.14 g of carbohydrates/100 g of CSM was reported; however, they found a high protein content of 16.4 ± 0.01 g and lipids 9.05 ± 0.1 g/100 g of CSM. They noted that the mucilage was contaminated with the seed itself. It is worth highlighting that the results obtained in this experimental research indicate a lower presence of compounds such as proteins, lipids and crude fiber which can affect the physicochemical properties of the final product.

Table 5. Proximal chemical composition of *S. hispanica* L. mucilage.

Sample	Crude Fiber (%)	Total CHOS (%)	Moisture (%)	Ashes (%)	Proteins (%)	Lipids (%)
1	45.10 ± 0.14 ^{c}	74.05 ± 0.54 ^{a}	12.78 ± 0.12 ^{c}	6.62 ± 0.20 ^{c}	5.44 ± 0.21 ^{c}	1.75 ±0.06 ^{d}
2	27.66 ± 0.29 ^{b}	77.19 ± 1.26 ^{b}	12.02 ± 0.04 ^{b}	6.04 ± 0.27 ^{a}	3.48 ± 0.04 ^{b}	0.48 ± 0.01 ^{a}
3	26.66 ± 0.31 ^{b}	78.12 ± 0.38 ^{b}	11.77 ± 0.23 ^{b}	6.19 ± 0.05 ^{b}	2.64 ± 0.05 ^{a}	0.98 ± 0.02 ^{c}
4	25.83 ± 0.14 ^{a}	73.68 ± 1.82 ^{a}	12.62 ± 0.06 ^{c}	6.44 ± 0.09 ^{c}	2.65 ± 0.04 ^{a}	0.56 ± 0.03 ^{b}
5	25.06 ± 0.08 ^{a}	77.89 ± 4.47 ^{b}	10.73 ± 0.16 ^{a}	6.06 ± 0.45 ^{a}	4.91 ± 0.04 ^{c}	0.55 ±0.04 ^{b}

All components are reported as g per 100 g of CSM. Different letters in the table indicate statistically significant differences ($\alpha = 0.05$).

García-Salcedo et al. [15] reported a high ash content of 11.28 ± 0.9 g/100 g of CSM and confirmed by means of a micrograph analysis the presence of protein bodies and fat globules. That is when purification becomes an alternative to not only achieve high levels of carbohydrates, but also low levels of the other components of the seed; however, the extraction process of mucilage becomes more expensive. A recent study presented the highest carbohydrate content with 93.06 ± 0.5 g, without reporting any type of fiber, 2.46 ± 0.02 g of protein, and 0.6 ± 0.1 g of lipids, with a low moisture content of 3.9 ± 0.3 g/100 g of CSM [23]. It should be noted that one of the advantages that ultracentrifugation offers compared to other CSM extraction studies is that it is an easy-to-scale operation and much lower cost compared to other emerging technologies.

3.3. Monosaccharide Profile of Chia Seed Mucilage

Table 6 shows the six major monosaccharides (xylose, glucose, glucuronic acid, arabinose, mannose and galactose) contents in chia mucilage seeds obtained at different hydration temperature and mechanical extraction conditions (samples 1 to 5). Sample 1 exhibited a monosaccharide profile characterized by high levels of xylose and glucose, whereas the contents of glucuronic acid, arabinose, mannose, and galactose were the lowest among all samples. In contrast, samples 2 and 3, processed at 75 °C, underwent a more intensive thermo-mechanical extraction that enhanced the detachment and solubilization of mucilage from the epidermal cell layers. The elevated temperature not only improved polysaccharide hydration but also promoted partial swelling and weakening of the seed coat matrix, facilitating the release of acidic hemicellulosic polysaccharide fractions containing glucuronic acid and neutral sugars associated with hemicelluloses. Consequently, these samples showed moderate increases in glucuronic acid, arabinose, and mannose, while maintaining xylose and glucose as the predominant carbohydrate components. The predominance of xylose together with arabinose and glucuronic acid is consistent with previous reports indicating that chia seed mucilage is mainly composed of glucuronoarabinoxylan-type polysaccharides [3,4,22].

Table 6. Monosaccharide profiles of experimental samples and molar ratios.

Sample	Xylose (%)	Glucose (%)	Glucuronic Acid (%)	Arabinose (%)	Mannose (%)	Galactose (%)	Molar Ratio Xyl:Glc:GlcA:Ara:Man:Gal
1	37.50 ± 0.41 ^{c}	24.22 ± 0.62 ^{d}	4.15 ± 0.30 ^{a}	7.53 ± 0.60 ^{a}	5.52 ± 0.21 ^{a}	6.10 ±0.16 ^{a}	1.00:0.54:0.09:0.20:0.12:0.14
2	36.00 ± 0.39 ^{b}	22.41 ± 0.38 ^{c}	6.50 ± 0.17 ^{e}	8.56 ± 0.47 ^{c}	7.53 ± 0.74 ^{c}	6.82 ± 0.91 ^{c}	1.00:0.52:0.14:0.24:0.17:0.16
3	38.26 ± 0.36 ^{d}	20.71 ± 0.18 ^{b}	6.32 ± 0.26 ^{d}	9.52 ± 0.25 ^{e}	8.73 ± 0.45 ^{e}	7.25 ± 0.27 ^{d}	1.00:0.45:0.13:0.25:0.19:0.16
4	40.53 ± 0.54 ^{e}	19.95 ± 0.25 ^{a}	5.13 ± 0.20 ^{c}	9.31 ± 0.49 ^{d}	7.71 ± 0.38 ^{d}	6.21 ± 0.33 ^{b}	1.00:0.41:0.10:0.23:0.16:0.13
5	35.68 ± 0.38 ^{a}	22.51 ± 0.17 ^{c}	5.00 ± 0.10 ^{b}	8.15 ± 0.35 ^{b}	9.71 ± 0.64 ^{b}	6.83 ±0.44 ^{c}	1.00:0.53:0.11:0.23:0.23:0.16

The values represent mean ± standard deviation (SD), n = 3. Means in columns with different letters differ significantly ($p \leq 0.05$). Xyl = xylose, Glc = glucose, GlcA = glucuronic acid, Ara = arabinose, Man = mannose, Gal = galactose.

Sample 4, extracted at 50 °C with 43.7 Hz and 50% screw restriction, demonstrated the highest mucilage extraction efficiency and minimal protein and lipid contents (Table 5). These conditions appear optimal for releasing the mucilaginous epidermal coating while minimizing disruption of deeper tissues. Accordingly, Sample 4 displayed a composition closely resembling purified chia gum, with xylose (40.53 ± 0.54) and glucose (19.95 ± 0.25) in proportions approaching the characteristic ≈ 2:1 ratio, a moderate amount of glucuronic acid (5.13 ± 0.20) consistent with reports for neutral/acidic gum fractions, and balanced quantities of arabinose, mannose, and galactose. This profile reflects a composition that is richer and structurally closer to the exudate described by [4], and the high-purity gum obtained by [22], while still retaining minor native components due to the absence of chemical purification. Finally, sample 5, obtained under maximum rotational speed (50.2 Hz) and 100% screw restriction at 25 °C, represented conditions of intense mechanical disruption with minimal thermal softening. These parameters favored the co-extraction of deeper structural polysaccharides such as mannans and galactans, which are less accessible under milder conditions. As a result, sample 5 showed the highest mannose content and the second-highest glucose content relative to the other experimental samples.

3.4. Molecular Weight (MW)

The average molecular weight obtained from CSM was shown in Table 7. The values of the MW were obtained of the five samples in the range of 5.39–37.81 × 10^4 kDa. The molecular weight distribution of samples depolymerized (CSP) for 0, 2, 4 and 8 h of degradation time were 2.34 × 10^3, 9.84 × 10^5, 6.78 × 10^5 and 2.67 × 10^5 kDa, respectively, were presented by Timilsena et al. [23].

Table 7. Molecular weight (MW) of chia seed mucilage.

Sample	Molecular Weight (kDa)
1	$5.39 \times 10^4 \pm 0.05$
2	$5.40 \times 10^4 \pm 0.04$
3	$20.88 \times 10^4 \pm 0.03$
4	$37.81 \times 10^4 \pm 0.015$
5	$34.04 \times 10^4 \pm 0.06$

The MW of CSM was significantly higher than that obtained by Timilsena et al. [24]. This difference could be due to the extraction method of chia seed mucilage, the process conditions, and to alternative methods of purifying polysaccharide. Separation efficiency allows for obtaining different molecular weights, if the intention is to apply it to micro or nano particulate systems.

3.5. Detection of Inorganic Nutrients

Elemental semi-quantitative analysis was performed on the five samples of mucilage by ±FRX. Mucilage samples 1, 2, 3, 4, and 5 showed Ca, Mg, K, and P as the main elements. The Ca^{2+}/P^{2+} ratios for samples 1, 2, 3, 4, and 5 were 2.74, 2.51, 1.18, 2.54, and 1.11, respectively.

3.6. Identification of Crystalline Structures of CSM by X-Ray Diffraction

Figure 4 shows the X-ray diffraction patterns for ashes of samples obtained in the optimal design. The main inorganic compounds in sample 4 (Figure 4a) were identified using the PDF program (Powder Diffraction File), which is available as a free download. For crystal structure identification, the minerals found in mucilage using X-ray fluorescence were used. Magnesium oxide (MgO), calcium phosphide (Ca_5P_8), potassium sulfide (K_2S), and potassium phosphide alpha (α-K_3P_1) were identified. In smaller quantities: K_4P_6, K_2S_3, and $CaCO_3$ were also present. The crystalline structures were identified using the powder diffraction file: MgO (PDF # 77-2364), Ca_5P_8 (PDF # 48-1825), K_2S (PDF # 65-3001), K_3P_{11} (PDF # 6-289), Ca_5P_8 (PDF # 74-0616), K_2S_3 (PDF # 71-0234), and $CaCO_3$ (PDF # 72-1650). $CaCO_3$ was identified in the chia mucilage, while MgO was found in chia flour [15]. The crystalline phases identified in sample 5 (Figure 4b) were MgO, $CaCO_3$, $KCaPO_4$, K_2S_3, $Ca_5P_{8,}$ and $CaSi_2$. $CaCO_{3,}$ MgO, and $K_4P_2O_8$ were identified in nopal [27]. Some differences were found between samples, which could be associated with the nature of the mucilage and changes in the extraction process conditions. These analyses were performed on all samples used in this study.

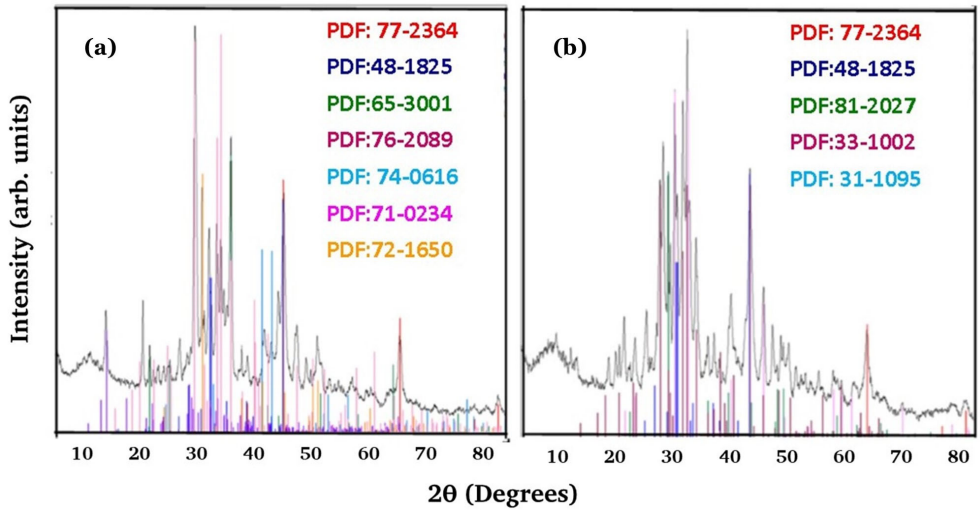


Figure 4. Effect of the extraction process conditions on X-ray diffffraction pattern of chia mucilage. (**a**) samples 4, 3, and 5; (**b**) samples 1 and 2.

3.7. Flow Properties of the Dried Mucilage

The real density of the powdered mucilage of the samples 1, 2, 3, 4, and 5 at the different extraction conditions was 0.795 ± 0.001, 0.771 ± 0.003, 0.758 ± 0.001, 0.747 ± 0.002, 0.730 ± 0.001 g/cc, respectively. García-Salcedo et al. [15] reported that the apparent density of chia seeds was 0.61 ± 0.01 g/cc. The values of the Carr index were in the range from 12 to 22%; this indicated that the mucilage is not compressible. The Hausner index was between 1.13 ± 0.02 and 1.28 ± 0.01, which means that all the mucilage samples show little settlement. The relationship between bulk density and compacted density provides a measure of the interactions between particles and the flow capacity. According to flow properties of the dried mucilage samples, it has the capacity to flow.

3.8. Morphological Characterization of CSM by Scanning Electron Microscopy

Figure 5 shows the SEM images taken at 50× of the hydrated seeds and mucilage at 1000×. The left column shows variations in seed hydrated morphology at 25, 50, and 75 °C.

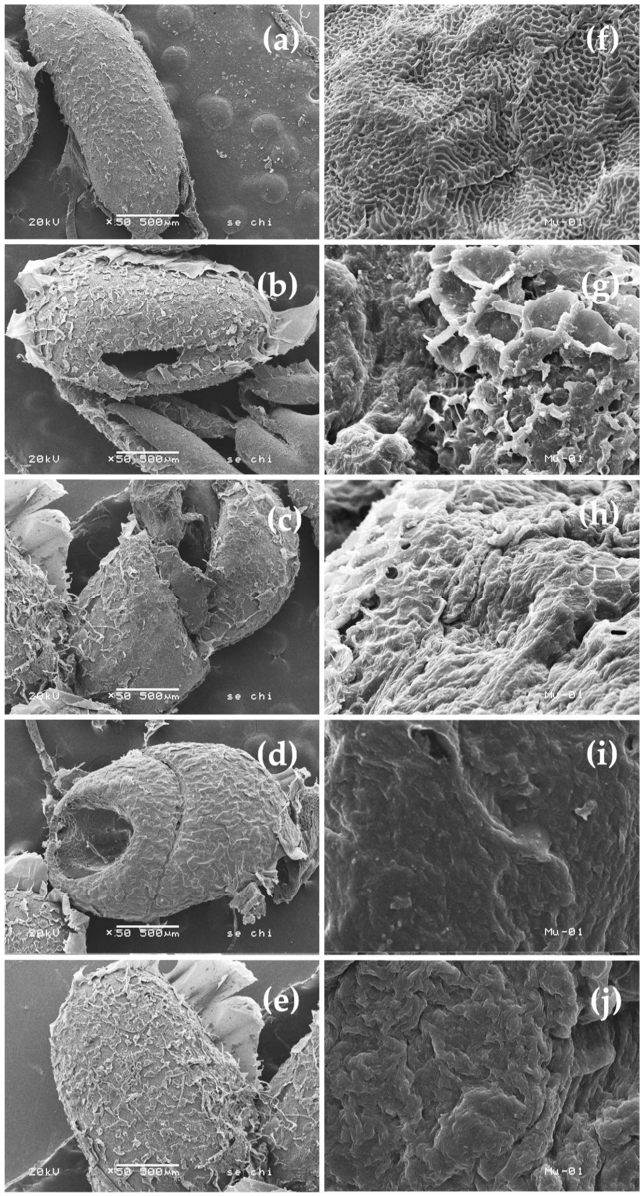


Figure 5. Micrographs of the hydrated seeds and extracted mucilage: the **left** column shows the hydrated seeds (50×), and the **right** column shows mucilage samples (1000×). Sample 1 (**a**,**f**), sample 2 (**b**,**g**), sample 3 (**c**,**h**), sample 4 (**d**,**i**) and sample 5 (**e**,**j**).

As can be seen, the temperature at 75 °C in the seeds caused rupture and exposure of their content, such as insoluble fiber, etc. The hydration at 50 °C for 5 min allowed observing that the mucilage crossed the pericarp of the seed, covering it entirely and becoming the densest cover over time; if the soaking time is overdone, the seed breaks. García-Salcedo et al. [15] presented images of the chia seed, exhibiting the pericarp structure and internal organization, as well as of the lyophilized mucilage. In Figure 5, the micrograph of the left column shows seeds at different temperatures (a) sample 1, (b) sample 2, (c) sample 3, (d) sample 4, and (e) sample 5. At 25 °C, there was a light exudation of the mucilage on the surface of the seed, and fiber strands were observed. In the right column, the mucilage sample 1 (Figure 5f) reveals on the surface a structure of polygonal isodiametric cells (HEX cells) corresponding to the epidermis covered with a thin film of mucilage. According to the microstructural analysis of [28], these polygonal cells make up the three layers of the epidermis and coincide with the structure identified in the mucilage fragment of sample 2 (Figure 5g) that corresponds to the insoluble fiber of the seed's epidermis. Sample 3 (Figure 5h) showed sections of insoluble fiber and other irregularities covered with mucilage. Undoubtedly, higher temperatures come to drag pieces of the insoluble fraction to be dragged due to the breaking of the seed. Mucilage sample 4 (Figure 5i) did not report insoluble fiber, but rather a thick corrugated matrix, while sample 5 (Figure 5j) showed a smoother and uniform surface.

3.9. Fourier Transform Infrared Spectroscopy (FTIR) Analysis

The IR spectrum of the chia mucilage (Figure 6) shows the chemical groups for peaks located at 4000 to 1500 cm^{-1} (Figure 6a) and from 1500 to 600 cm^{-1} (Figure 6b).

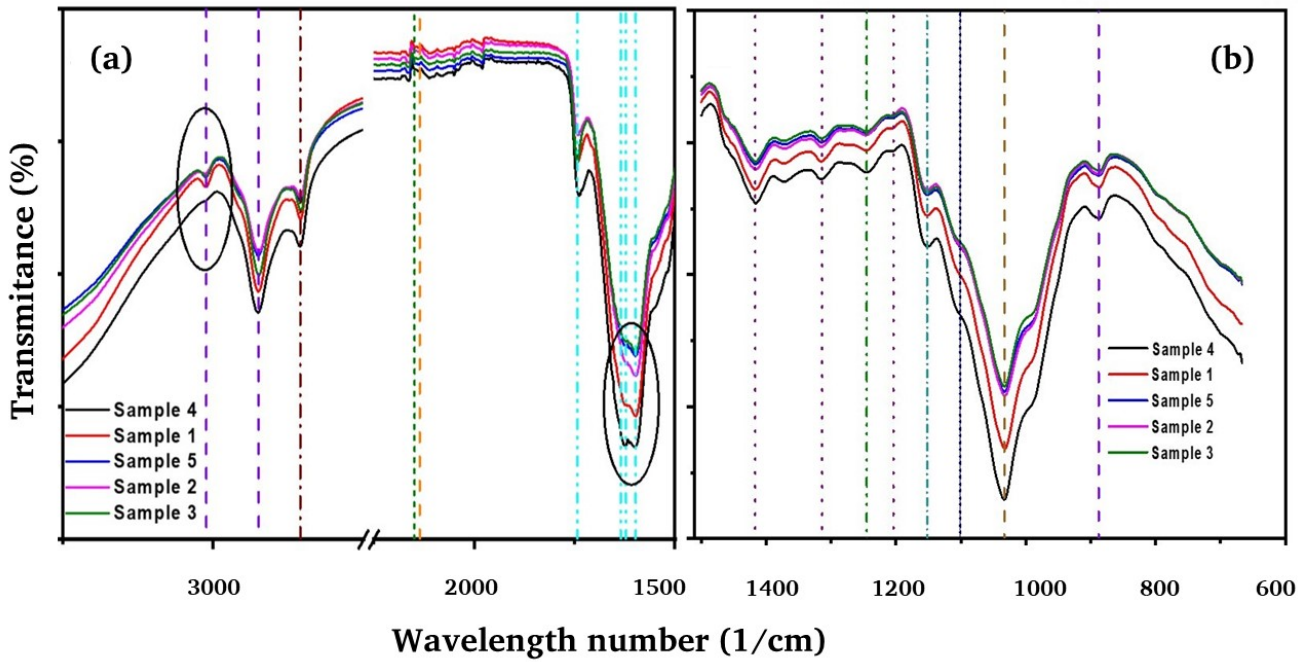


Figure 6. IR spectrum of chia mucilage at different extraction conditions. (**a**) IR from 4000 at 1500 cm^{-1}; (**b**) IR from 1500 to 600 cm^{-1}.

The bands at 2924 cm^{-1} and 3011 cm^{-1} showed stretching vibration in a pyranose group that disappears in sample 4 (Figure 6a). The band at 1417 cm^{-1} is assigned to the –COOH group is related to flexion vibration, and at 1598 $cm^{-1,}$ with stretching vibration, both in uronic acid. This group was also assigned at 1622 cm^{-1} was predominant in sample 4, with stretching vibration in the mannose ring. This means that the centrifuge at the optimal conditions allows for recovery of D-mannose. The chemical group –OH at 1101 cm^{-1} is a predominant peak, and at 3291 cm^{-1} with stretching vibration. The C-O group at 1245 cm^{-1}

and 2149 cm^{-1} corresponds to stretching vibrations. The C-O-C group at 1033 cm^{-1} with stretching vibrations of the pyranose ring and bound at position 1–4 for the glycosidic bond. The group –CH present in 888 cm^{-1} corresponds to anomeric deformation β-CH and glycosidic bond. It is attributed to glucopyranose and xylopyranose. These groups have also been identified by [22,29].

3.10. Refraction Index, pH, and Particle Size in Dispersion

The pH of the mucilage sample obtained under optimal conditions (sample 4) in colloidal dispersion at concentrations of 0.125%, 0.25%, 0.5%, and 1% (*w*/*w*) was 6.01 ± 0.11, 6.14 ± 0.09, 6.24 ± 0.18, and 6.43 ± 0.2, respectively. The pH averages 6.12 ± 0.15 and does not change at different concentrations or over time. The refraction index increases with mucilage concentration, ranging from 1.3325 ± 0.05 to 1.3360 ± 0.02. The particle size (PS) of mucilage dispersion at 0.5% for samples 1, 2, 3, 4, and 5 was 15.52 ± 0.13; 15.74 ± 0.31; 15.26 ±0.21; 15.28 ± 0.22, and 15.80 ± 0.11 μm, respectively.

3.11. Aggregation Stability of Mucilage Dispersions

The Zeta Potential (ζ) values from mucilage dispersion at 0.5% for samples 1, 2, 3, 4, and 5 were 4.6 ± 0.1; 5.3 ± 0.1; 9.5 ±0.2; 9.7 ± 0.3, and 12.3 ± 0.2 mV, at a pH of 6.0. These changes in the ζ can be attributed to the ionization of the carboxyl group contained in uronic acids [22]. For sample 4, the ζ of the particles in dispersion at concentrations 1, 0.5, and 0.25% after 1 day of preparation presented the following values: −44.5 ± 1.2, −18.3 ± 0.7, and −16.6 ± 0.5. At ζ majors, the particles repel more easily due to their electrical charges; there is less aggregation among themselves. On day 5, the charges were: −26.4 ± 1.8, −16.5 ± 0.6, and 5.7 ± 0.3, respectively. The magnitude of the charges decreases as time goes by; this is due to the ζ has a maximum value on the surface of the particle and decreases gradually, approaching zero as the distance between particles increases. A colloid with a negative net charge and an oppositely charged surrounding atmosphere produces an electrical potential different from zero, close to the interface and relative to the suspension, according to [29].

3.12. Rheological Analysis of Chia Mucilage

Figure 7 shows that the storage modulus (G′) was higher than the loss modulus (G″), under different extraction conditions and mucilage concentrations. The highest values of G′ and G″ were observed for sample 3 at 1% (*w*/*w*), while the lowest were found for sample 2 at 0.25% (*w*/*w*). The G′ curves for samples 1, 2, and 5 at 1% (*w*/*w*) showed similar trends and magnitudes in the frequency sweep. Similarly, the samples 1, 3, and 5 at 0.5% (*w*/*w*) for G′ exhibited comparable trends. These results suggest that dispersed and swollen microgel particles of mucilage form a "weak gel" which is responsible for this rheological behavior. The data reported by [2,24] showed similar behavior. Goh et al. [30] reports that the behavior of weak gel networks is attributed to the elasticity of the physical contact between neighboring particles. In contrast, the sample 4 at 1% and 0.25% (*w*/*w*) showed the same behavior for G′ (Figure 7a). Additionally, G″ for samples 1 and 2 from 0.25% to 1% (*w*/*w*) presented the same exponential trend (see Figure 7b). Sample 4 from 0.25% to 1% (*w*/*w*) showed a nonlinear trend for both G′ and G″. The complex viscosity of the samples was measured, and the behavior was modeled using the Power Law. The methodology was used to solve the model and obtain the consistency index (K), and the flow behavior index (n).

Table 8 shows the consistency index (K) and flow behavior index (n) calculated for the samples in the optimal design. All the samples showed pseudoplastic behavior until a maximum limit of shear rate [31] mention that the consistency index and flow behavior index for chia mucilage were reported to be 0.12 $Pa{\cdot}s^n$ and 0.14, respectively. CSM solution

showed values of n < 1, which indicates the pseudoplastic and shear-thinning behavior of chia mucilage. This is consistent with the present research study.

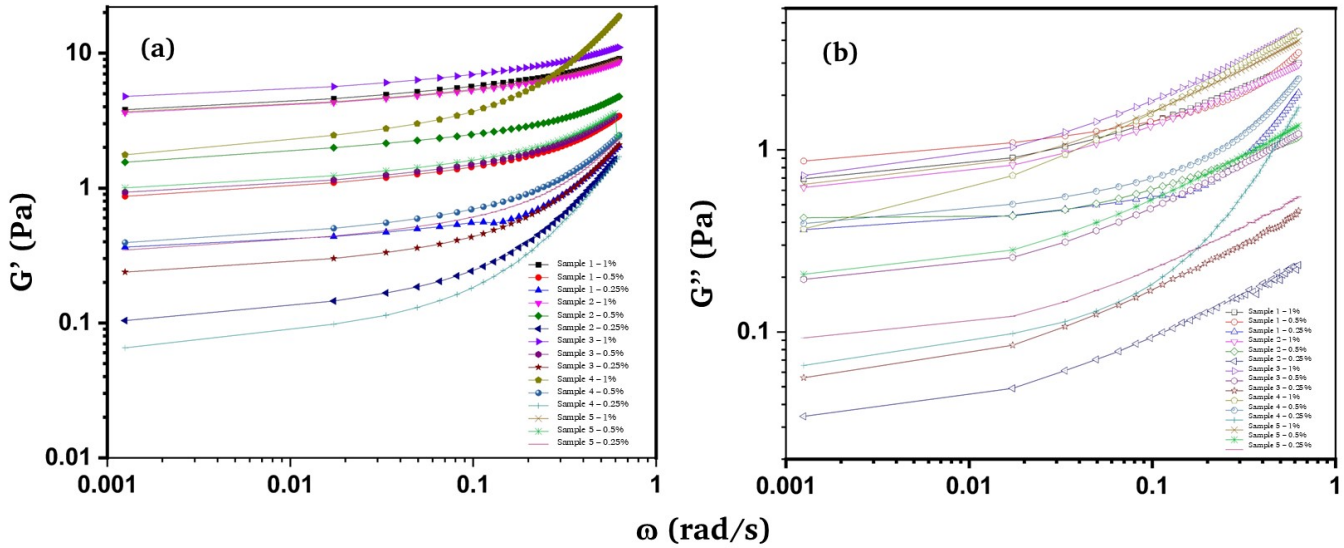


Figure 7. Mechanical spectra of G′ (**a**) and G″ (**b**) of chia mucilage versus frequency sweep at different extraction conditions (S1, S2, S3, S4, and S5) and concentrations of 1%, 0.5% and 0.25% (*w*/*w*).

Table 8. Rheological parameters obtained for the different chia mucilage samples at different extraction conditions and concentrations.

Sample	K (Pa s^n)	n (–)
S1 at 1%	0.241	0.198
S1 at 0.5%	0.059	0.192
S1 at 0.25%	0.019	0.144
S2 at 1%	0.229	0.201
S2 at 0.5%	0.067	0.206
S2 at 0.25%	0.02	0.221
S3 at 1%	0.285	0.186
S3 at 0.5%	0.067	0.206
S3 at 0.25%	0.02	0.221
S4 at 1%	0.122	0.194
S4 at 0.5%	0.034	0.229
S4 at 0.25%	0.012	0.325
S5 at 1%	0.257	0.223
S5 at 0.5%	0.073	0.21
S5 at 0.25%	0.03	0.233

The ANOVA performed reveals that the consistency index has a significant effect ($p \leq 0.05$) given by the concentration of chia mucilage, regardless of the type of sample analyzed ($p > 0.05$), for the values obtained for the flow behavior index, no statistically significant effect was observed due to the independent factors ($p > 0.05$). These results are important because they are related to the possible applications of this material. Research regarding viscosity in formulations with gum concentrations between 0.25 and 1% (*w*/*w*). The concentrations exhibited non-Newtonian rheology [31] due to the large quantity of hydrocolloid molecules in suspension that confer pseudo-plastic behavior. Santana et al. [7] studied the rheology of the CSM and reported pseudoplasticity at low concentrations, due to the presence of soft microgel particles, which present sensitivity even at low shear and concentration.

4. Conclusions

Mucilage can be efficiently extracted using centrifugation as a method of mixture separation. Increasing the turning speed and the restriction screw in the centrifuge promoted decreased mucilage contamination with lipids, proteins, insoluble fiber, and other compo-

nents. The studied variables including the relationship between hydration temperature, exudation time, and seed: water ratio, are important for understanding and affecting the extraction yield and efficiency of CSM. Optimal process conditions were 50 °C, 46 Hz of turning speed, and 100% screw restriction. Hydration temperature and mechanical processing intensity (rotational speed and screw restriction) significantly influenced the monosaccharide composition of *S. hispanica* L. mucilage, demonstrating that extraction conditions directly modulate the structural and chemical characteristics of the recovered polysaccharide. The mucilage exhibited good flow properties, with particle sizes ranging from intermediate to fine. Its chemical composition was primarily carbohydrates, as confirmed by micrographs and the identification of its chemical nature. The predominant functional groups were –COOH, characteristic of uronic acid, and mannose ring; –OH from carbohydrates; –CH corresponding to glucopyranose and xylopyranose, and C-OC, corresponding to pyranose. The mucilage can contribute to minerals such as K, Ca, Mg, and P. The presence of ions changes its charge potential when it is dispersed in water due to the degree of ionization of the –COOH, which interferes with the formation of microgels that also have an impact on its rheological behavior (these minerals can also be co-extracted by aqueous extraction). Breaking the seeds causes the detachment of other components, altering their composition and properties, and thus increasing mucilage contamination. Changes in the chemical composition and structural conformation of the mucilage due to extraction influence its physicochemical properties and phase behavior. Controlling extraction conditions improves mucilage properties, increasing its technological applications. Future research may address comprehensive profiling of minor constituents (phenolics, flavonoids, or other low-molecular-weight compounds), in combination with the process–structure–function relationships established in this work, to further support application-oriented design of chia-derived hydrocolloids.

Author Contributions: F.R.C.-G.: investigation, methodology, formal analysis, and writing—original draft. R.M.G.-R.: supervision and writing—review and editing. I.R.-M.: investigation and methodology. J.L.S.-M.: investigation and methodology. C.T.Q.-B.: supervision and review. A.R.-M.: investigation and methodology. E.G.-C.: conceptualization, methodology, writing—review and editing, project administration, funding acquisition, and approval of final document. All authors have read and agreed to the published version of the manuscript.

Funding: This research received no external funding.

Data Availability Statement: The data presented in this study are available on request from the corresponding author. The data are not publicly available due to privacy and ethical restrictions.

Acknowledgments: Frida Rosalía Cornejo-García is grateful for the doctoral scholarship support from SECIHTI-México. The authors also thank M.I. Alicia del Real López for her assistance in the SEM imaging process.

Conflicts of Interest: The authors declare no conflicts of interest.

References

1. Muñoz, L.A.; Cobos, A.; Diaz, O.; Aguilera, J.M. Chia Seeds: Microstructure, Mucilage Extraction and Hydration. *J. Food Eng.* **2012**, *108*, 216–224. [CrossRef]
2. Capitani, M.I.; Ixtaina, V.Y.; Nolasco, S.M.; Tomás, M.C. Microstructure, Chemical Composition and Mucilage Exudation of Chia (*Salvia hispanica* L.) Nutlets from Argentina. *J. Sci. Food Agric.* **2013**, *93*, 3856–3862. [CrossRef]
3. Punia, S.; Dhull, S.B. Chia Seed (*Salvia hispanica* L.) Mucilage (a Heteropolysaccharide): Functional, Thermal, Rheological Behaviour and Its Utilization. *Int. J. Biol. Macromol.* **2019**, *140*, 1084–1090. [CrossRef] [PubMed]
4. Lin, K.-Y.; Daniel, J.R.; Whistler, R.L. Structure of Chia Seed Polysaccharide Exudate. *Carbohydr. Polym.* **1994**, *23*, 13–18. [CrossRef]
5. Mensah, E.O.; Oludipe, E.O.; Gebremeskal, Y.H.; Nadtochii, L.A.; Baranenko, D. Evaluation of Extraction Techniques for Chia Seed Mucilage; A Review on the Structural Composition, Physicochemical Properties and Applications. *Food Hydrocoll.* **2024**, *153*, 110051. [CrossRef]

6. da Silveira Ramos, I.F.; Magalhães, L.M.; do O Pessoa, C.; Pinheiro Ferreira, P.M.; dos Santos Rizzo, M.; Osajima, J.A.; Silva-Filho, E.C.; Nunes, C.; Raposo, F.; Coimbra, M.A.; et al. New Properties of Chia Seed Mucilage (*Salvia hispanica* L.) and Potential Application in Cosmetic and Pharmaceutical Products. *Ind. Crops Prod.* **2021**, *171*, 113981. [CrossRef]
7. Santana, R.D.C.; Tavares, M.B.F.; Coimbra, J.S.D.R.; Martins, M.A.; Sousa, R.D.C.S.D. Effect of Extraction Conditions of Chia (*Salvia hispanica* L.) Mucilage on Its Chemical, Rheological, and Emulsifying Properties. *ACS Food Sci. Technol.* **2025**, *5*, 687–694. [CrossRef]
8. Chiang, J.H.; Ong, D.S.M.; Ng, F.S.K.; Hua, X.Y.; Tay, W.L.W.; Henry, C.J. Application of Chia (*Salvia hispanica*) Mucilage as an Ingredient Replacer in Foods. *Trends Food Sci. Technol.* **2021**, *115*, 105–116. [CrossRef]
9. Tan, Q.Y.; Solanki, D.; Badin, R.; Prakash, S. Comparing Conventional and Novel Extraction Methods for Chia Seed Mucilage as a Sustainable Vegan Thickening Agent. *Sustain. Food Technol.* **2025**, *3*, 456–469. [CrossRef]
10. Solanki, D.; Oey, I.; Prakash, S.; Bhandari, B.; Sahu, J.K. Prospects of Using Non-Thermal Technologies for Chia Seed Mucilage Extraction. *Sustain. Food Technol.* **2024**, *2*, 993–1010. [CrossRef]
11. Silva, L.A.; Sinnecker, P.; Cavalari, A.A.; Sato, A.C.K.; Perrechil, F.A. Extraction of Chia Seed Mucilage: Effect of Ultrasound Application. *Food Chem. Adv.* **2022**, *1*, 100024. [CrossRef]
12. Solanki, D.; Punzalan, J.M.; Oey, I.; Meriaux, A.; Gordon, K.C.; Bhandari, B.; Sahu, J.K.; Prakash, S. Non-Thermal Extraction and Modification of Chia Seed Mucilage Using Pulsed Electric Field. *Food Hydrocoll.* **2026**, *172*, 111954. [CrossRef]
13. Chen, J.; Ge, W.; Wang, P.; Lv, W.; Wang, H. PEG-Based-Ultrasound-Microwave Synergistic Extraction of Mucilage Polysaccharides from Chia Seed: Structural Characterization and Bioactivity. *Int. J. Biol. Macromol.* **2024**, *283*, 138057. [CrossRef] [PubMed]
14. Bhatkar, N.S.; Kaimal, A.M.; Shirkole, S.S.; Sahoo, A.K. Optimization of Microwave Assisted Extraction of Mucilage from Garden Cress Seeds and Its Characterization. *Int. J. Biol. Macromol.* **2025**, *320*, 145997. [CrossRef] [PubMed]
15. García-Salcedo, Á.J.; Torres-Vargas, O.L.; del Real, A.; Contreras-Jiménez, B.; Rodriguez-Garcia, M.E. Pasting, Viscoelastic, and Physicochemical Properties of Chia (*Salvia hispanica* L.) Flour and Mucilage. *Food Struct.* **2018**, *16*, 59–66. [CrossRef]
16. Karimi, N.; Abbasi, H.; Nasr-Esfahani, M. High-Intensity Short-Term Electrical Pulses Pretreatment on Efficiency and Functional Characteristics of Extracted Chia Seed Mucilage: Optimization through Response Surface Methodology. *Innov. Food Sci. Emerg. Technol.* **2025**, *100*, 103915. [CrossRef]
17. Dick, M.; Costa, T.M.H.; Gomaa, A.; Subirade, M.; Rios, A.D.O.; Flôres, S.H. Edible Film Production from Chia Seed Mucilage: Effect of Glycerol Concentration on Its Physicochemical and Mechanical Properties. *Carbohydr. Polym.* **2015**, *130*, 198–205. [CrossRef]
18. Vera Candioti, L.; De Zan, M.M.; Cámara, M.S.; Goicoechea, H.C. Experimental Design and Multiple Response Optimization. Using the Desirability Function in Analytical Methods Development. *Talanta* **2014**, *124*, 123–138. [CrossRef]
19. Orifici, S.C.; Capitani, M.I.; Tomás, M.C.; Nolasco, S.M. Optimization of Mucilage Extraction from Chia Seeds (*Salvia hispanica* L.) Using Response Surface Methodology. *J. Sci. Food Agric.* **2018**, *98*, 4495–4500. [CrossRef]
20. ASTM. *Libro Annual de Normas ASTM. Sección 11. Agua y Tecnología Ambiental*; Agua. © Attribution Non-Commercial (BY-NC); ASTM Int.: West Conshohocken, PA, USA, 2012; Volume 11.
21. AOAC International; Guideline Working Group. AOAC International guidelines for validation of botanical identification methods. *J. AOAC Int.* **2012**, *95*, 268–272. [CrossRef] [PubMed]
22. Timilsena, Y.P.; Adhikari, R.; Kasapis, S.; Adhikari, B. Molecular and Functional Characteristics of Purified Gum from Australian Chia Seeds. *Carbohydr. Polym.* **2016**, *136*, 128–136. [CrossRef] [PubMed]
23. Timilsena, Y.P.; Adhikari, R.; Kasapis, S.; Adhikari, B. Rheological and Microstructural Properties of the Chia Seed Polysaccharide. *Int. J. Biol. Macromol.* **2015**, *81*, 991–999. [CrossRef]
24. Masuelli, M.A. Intrinsic Viscosity Determination of High Molecular Weight Biopolymers by Different Plot Methods. Chia Gum Case. *J. Polym. Biopolym. Phys. Chem.* **2018**, *6*, 13–25. [CrossRef]
25. Londoño-Restrepo, S.M.; Rincón-Londoño, N.; Contreras-Padilla, M.; Millan-Malo, B.M.; Rodriguez-Garcia, M.E. Morphological, Structural, Thermal, Compositional, Vibrational, and Pasting Characterization of White, Yellow, and Purple Arracacha Lego-like Starches and Flours (*Arracacia xanthorrhiza*). *Int. J. Biol. Macromol.* **2018**, *113*, 1188–1197. [CrossRef] [PubMed]
26. Contreras-Jimenez, B.; Gaytan-Martinez, M.; Morales-Sanchez, E.; De Dios Figueroa-Cardenas, J.; Pless, R.; Gonzalez-Jasso, E.; Mendez-Montealvo, G.; Velazquez, G. Effects of Tempering Time, $Ca(OH)_2$ Concentration, and Particle Size on the Rheological Properties of Extruded Corn Flour. *Cereal Chem.* **2017**, *94*, 230–236. [CrossRef]
27. Contreras-Padilla, M.; Rivera-Muñoz, E.M.; Gutiérrez-Cortez, E.; del López, A.R.; Rodríguez-García, M.E. Characterization of Crystalline Structures in *Opuntia ficus-indica*. *J. Biol. Phys.* **2015**, *41*, 99–112. [CrossRef] [PubMed]
28. de la Paz Salgado-Cruz, M.; Calderón-Domínguez, G.; Chanona-Pérez, J.; Farrera-Rebollo, R.R.; Méndez-Méndez, J.V.; Díaz-Ramírez, M. Chia (*Salvia hispanica* L.) Seed Mucilage Release Characterisation. A Microstructural and Image Analysis Study. *Ind. Crops Prod.* **2013**, *51*, 453–462. [CrossRef]
29. Timilsena, Y.P.; Wang, B.; Adhikari, R.; Adhikari, B. Preparation and Characterization of Chia Seed Protein Isolate-Chia Seed Gum Complex Coacervates. *Food Hydrocoll.* **2015**, *52*, 554–563. [CrossRef]

30. Goh, K.K.T.; Matia-Merino, L.; Chiang, J.H.; Quek, R.; Soh, S.J.B.; Lentle, R.G. The Physico-Chemical Properties of Chia Seed Polysaccharide and Its Microgel Dispersion Rheology. *Carbohydr. Polym.* **2016**, *149*, 297–307. [CrossRef]
31. Guiotto, E.N.; Capitani, M.I.; Nolasco, S.M.; Tomás, M.C. Stability of Oil-in-Water Emulsions with Sunflower (*Helianthus annuus* L.) and Chia (*Salvia hispanica* L.) By-Products. *JAOCS J. Am. Oil Chem. Soc.* **2016**, *93*, 133–143. [CrossRef]

Disclaimer/Publisher's Note: The statements, opinions and data contained in all publications are solely those of the individual author(s) and contributor(s) and not of MDPI and/or the editor(s). MDPI and/or the editor(s) disclaim responsibility for any injury to people or property resulting from any ideas, methods, instructions or products referred to in the content.